Geotechnical and Geophysical Site Characterisation 5 – Lehane, Acosta-Martínez & Kelly (Eds)

Use of Geophysical Logs to Map Aquifers Electrofacies

R. Macari & A. S. P. Peixoto
UNESP – Univ Estadual Paulista, Dept. Civil and Environmental Engineering, Bauru, Brazil

G. G. Nery
Hydrolog Serviços de Perfilagens Ltda., Bauru, Brazil

ABSTRACT: Map of geophysical parameters in different depth and their corresponding geological interpretations are analyzed based on an automatic geostatistical method to aquifers electrofacies identification using geophysical well logging curves of electrical resistivity, gamma ray and sonic transit time. The methodology for the spatial analysis of the variability of petrophysical characteristics considering their borehole geophysical responses, useful in oil industry, is extended here in water research. For that, they were used 65 geophysical logs scattered throughout the metropolitan region of São Paulo (Brazil) carried on between 1997 and 2012. In addition, the combined use of these three parameters has led to a better understanding of the subsurface rocks in the complex stratigraphy of Paleogene São Paulo Basin, Brazil, in order to future projects of planning groundwater wells.

1 INTRODUCTION

The city of São Paulo is fully urbanized and so it has no exposed geological outcrops making it difficult to study the subsoil. Thus, the use of existing data on artesian wells can help studies for urban planning, building construction and underground water extraction. That city is one of the largest urban centers of the Planet and it suffered an unprecedented water crisis in recent years leading to the necessity of choosing cost-effectively solutions.

The use of geophysical logs in groundwater wells is a commonplace and often essential to improve the water flow. In fact, after the construction of the well, the test results are stored. However, a better destination for them would be the use to plot 2D / 3D map information in order to help the geological knowledge of the exploited areas.

It is presented methodology using well logging data and ordinary softwares in order to better plan the construction of artesian wells leading to increase the flow of the artesian wells. The aquifers electrofacies were identified based on geophysical well logging curves of electrical resistivity, gamma ray and transit time of 65 well logs performed between the years of 1997 and 2012.

Also this work aims a better understanding of the subsurface layers in the basin of São Paulo, quite complicated stratigraphy, helping in better visualization and project planning of wells for groundwater extraction in the state capital.

2 METHODOLOGY

2.1 *Theoretical concepts*

According to Kearney et al (2013), the gamma rays are pure electromagnetic radiation released from excited nucleus during disintegrations and can be obtained by scintillation sensors. The gamma ray profile is one of the best indicators of lithological sedimentary rocks. The most important hydrogeological application of the technique is the identification and quantification of clay intervals choice of appropriate intervals for the placement of filters in groundwater wells. The American Petroleum Institute (API) normalized the gamma ray measurement as API unit.

A gamma ray shale index, I_{GR}, for a given layer is defined by Equation 1:

$$I_{GR} = \frac{(GR - GR_{cl})}{(GR_{sh} - GR_{cl})} \quad (1)$$

where GR = log response in the zone of interest, API units; GR_{cl} = log response in clean beds, API units; and GR_{sh} = log response in shale beds, API units

The induction logging provides the resistivity measurements in two ways: induction (DIR) and short normal (SN).

The DIR is obtained as follows: the surrounding rock is energized by an electromagnetic field of approximately 20 kHz, which generates currents by

electromagnetic induction. The secondary electromagnetic field created is recorded in a receiver that allows a direct estimate of the apparent resistivity with the unit in ohm-m.

The test use four coils, two transmission and two reception. The induced electromagnetic field flows in circular paths around the borehole. Such an arrangement provides a depth of penetration of about twice the transmitter-receiver separation.

The short normal, SN, is obtained as follows: a constant current is sent between a transmitter electrode, A, and the receiver electrode, B. It creates current lines crossing a certain amount of mud and rock. The tool reads the potential difference between the measuring electrodes M and N.

The borehole compensated sonic (BCS) also known as the continuous velocity or acoustic log, determines the seismic velocities of the formations traversed. The sonde normally contains two receivers about 0.30m apart and an acoustic source some 0.9–1.5m from the nearest receiver, Kearney et al (2013). These waves propagate in 3D shape inside the well and the formation. They are captured by an receiver located at a fixed distance from the transmitter. These receptors basically read the time between emission and arrival of the ultrasonic wave (transit time, DT) in μs/ft, as standardized by the API (e.g. 3.28 x 10^{-6} s/m).

2.2 *Study area*

The study area is located in the São Paulo Basin, Paleogene Age (Figure 1). The most wells are located between the Tietê River and the Pinheiros River, (Figure 2).

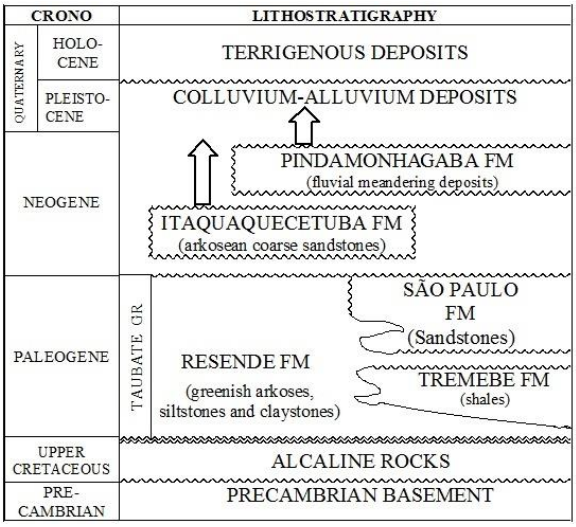

Figure 1. Stratigraphic Column São Paulo Basin. Modified of Riccomini et al (1989).

The typical log example of Figure 3 shows the high variability of the geology in the area with successive high-low values of transit time, resistivity and gamma anomalies peaks, as result of clay and sandy lenses. Below 110 meters there is altered basement igneous rock, visible by the low values of transit time, e.g. lower than 70 μsc/ft (2.3 x 10^{-4} s/m).

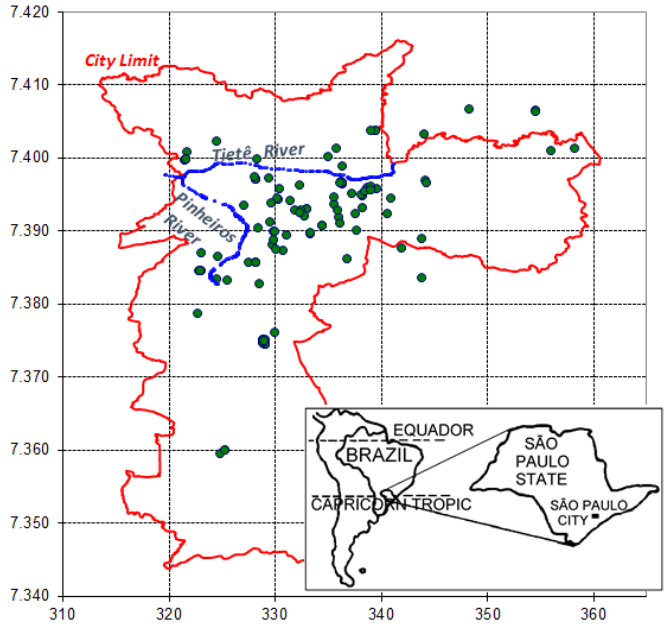

Figure 2. Location Map of São Paulo Wells Drilled

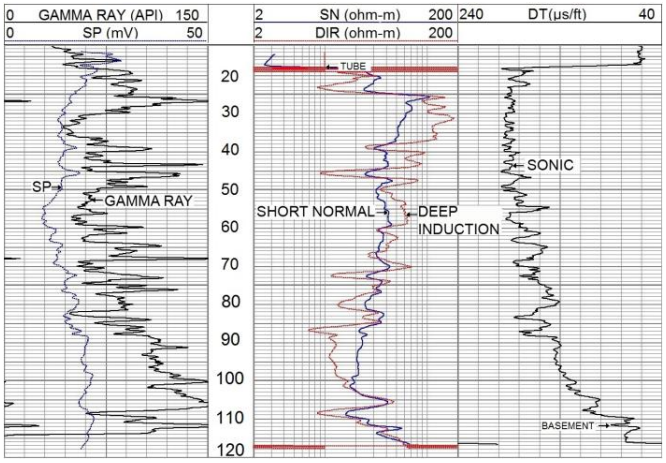

Figure 3. Typical Log in the São Paulo Basin.

The dashed line in Figure 4 shows the top of the crystalline rocks, since most of the logged well was drilled through the sedimentary layer. According to Takira (1991), the maximum continuous thickness of sediments in the is 250 meters in that place, but Figure 4 shows at most 185 meters of sediment.

The recent origin of the basin with discontinuous, unconsolidated and lenticular layers became quite complex geology and the establishment of a correlation between the logs a difficult task.

2.1 *Database*

The files of all 65 logs have been converted from the acquisition format (db) to Las text format (LAS - Log Ascii Standard) compatible with commercial

spreadsheet software. An example of spreadsheet used is detailed in Table 1.

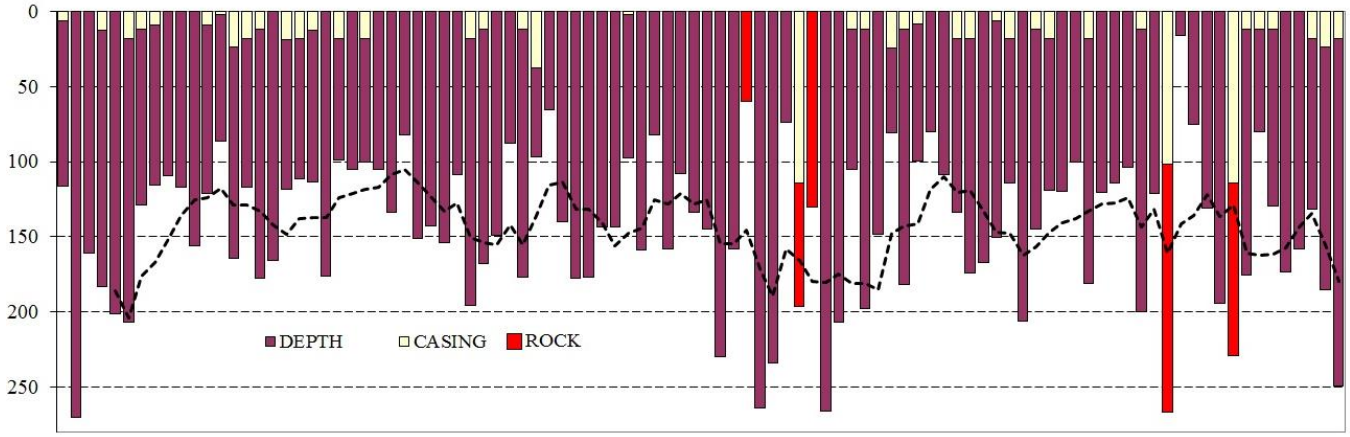

Figure 4. Depths (m) of the 65 wells used.

Table 1. Spreadsheet used in database

WELL nr	LOGS	DEPTH (m)	UTME	UTMN
Number given to logging.	IEL and GR (All Wells); DT	Depth reached.	UTM coordinates	

DIR (xm)	GR (xm)	DT (xm)	DIR (n)... GR (n) etc.
Resistivity value at the depth of "x" meter (ohm-m)	Value of Gamma Ray at the depth of "x" meter (GAPI).	Value of the Sonic Transit Time at the depth of "x" meter (μs/ft).	And so on according to the same scheme.

Induction logging and gamma ray datas were avaliable in all analysed wells but not all had sonic logging. In this way, the type of tool was considered in the analyzes. The wells were identified by number well (nr), the reached depth and UTM coordinate. It was done a separeted collumn for each meter depth of the values of induction resistivity, gamma ray and sonic.

The deep resistivity values of induction (DIR) above 200 ohm-m were set as 200ohm.m for interpolation the purposes, since resistivity changes above that value has little geological significance. The maps has been limited up to coordinate UTM 400,000 although some outliers wells located above this coordinate has been used for sake of interpolations.

3 MAPS

Maps of resistivity values, DIR (ohm-m), gamma rays, GR (GAPI) and transit time, DT (μs/ft) were done at each 10 meter depth from the top of layers. Neighboring wells correlation scale ranges were chosen in accordance to authors experience in the field, as seen in Table 2.

The Figures 5 show an example of 50m depth results from Krigging interpolation method according to Sturaro & Landim (1997) for the three curves resistivity values (DIR), gamma rays (GR) and transit time (DT).

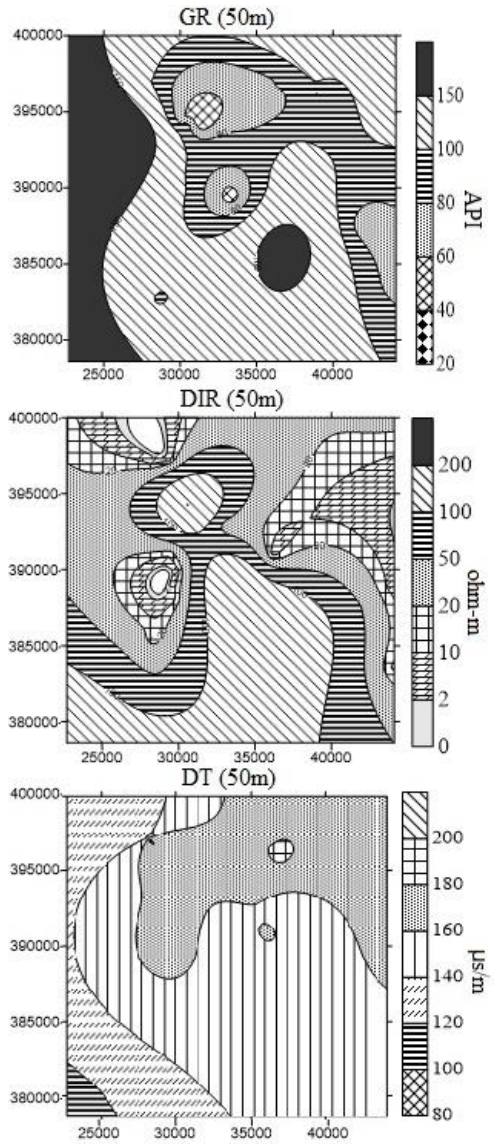

Figure 5. Example of Electrofacial Maps at 50 meters depth.

Table 2. Correlation between Gamma Ray, Transit Time and Deep Resistivity, range and lithology.

GAMMA RAY - GR		SONIC TRANSIT TIME - DT	
GAPI	INTERPRETED LITHOLOGY	μs/ft	INTERPRETED LITHOLOGY
40 - 60	Clean Sand	60 - 80	Well consolidated rock or sediment
60 - 80	Clay Sand	80 - 100	Consolidated sandstone or weathered rock
80- 100	Very Clayey Sand / Shale	100 - 120	Unconsolidated sandstone and clay
100-150	Shale/Clay/ Arkosic Sandstone	120 - 140	Low consolidated sediment
> 150	Arkosic Sandstone	140 - 160	Very low consolidated sediment
INDUCTION DEEP RESISTIVITY - DIR			
Ohm-m	INTERPRETED LITHOLOGY	Ohm-m	INTERPRETED LITHOLOGY
0 - 2	Clay/Shale	50 - 100	Water Sandstone
2 - 10	Sandy Clay	100 - 200	Water Sandstone or weathered rock
10 - 20	Sandstone clay		
20 - 50	Sandstone	> 200	Basement Rock or dry sandstone

4 ANALYSIS OF RESULTS

Clays, silts and fine clayey arkosic sands, with occurrences of coarse sand and fine gravel, compose the lithology of sedimentary basin of São Paulo. These sediments are textural and mineralogical immature. The coarser fractions are mainly in the central part of the basin.
Considering the probe samples and taking into account the low level of total salts in water, it was carried out the following analysis for each map.

4.1 *Gamma Ray*

The Figure 6 shows the gamma ray values maps. The higher GAPI values observed at all depths demonstrate the predominance of immature sediments. Arkosic sandstones are explained by the high gamma values due to ^{40}K (radiative) of potassium feldspar. It is almost difficult to correlate the presence of sand based only in low GAPI. There is a sand trend to north of studied area and possibly a sandy body delimited to 40 meters in the northern portion center. This layer has a clayey intercalation after 80 meters depth. It turns to be sandy at 90 meters depth, almost disappearing at 100 meters depth.

4.2 *Deep Induction*

The analyses of the induction curves show higher values (100-200 ohm-m) in the SW portion of the map, Figure 7, due to the presence of the crystalline basement in place. In this way, DIR is the profile that best characterizes the area because it is not be influenced by the lack of maturity of the sediments.

The lower resistivity values (2-50 ohm-m), between 50 and 70 meters lead to a possibly existence of clay material. At 80 meters there is high resistivity layer (possibly a sandy layer) that does not have continuity at greater depths. The portion of NW has consistently low values indicating more clay material for all depths. The SE portion shows intermediate values interlayered with sandy layers in sandy clay.

In addition, the alternating layers with high resistivity (sandy layers) in the central part of maps can be noted in Figure 7. Noteworthy is a high resistivity layer, with low gamma ray and high transit time up to 60 meters. There is a sandy layer with a good log correlation. Bellow 70 meters, the increase of gamma values increase with decrease of resistivity.

4.3 *Borehole Compensated Sonic (BCS)*

In the depth up to 30m, the high transit time values indicate low textural maturity and high porosity, map DT 20 of Figure 8. The reduction of the transit time values in the SW direction (below 100 μs/ft) suggests a change in to the crystalline basement, map DT100 of Figure 8.

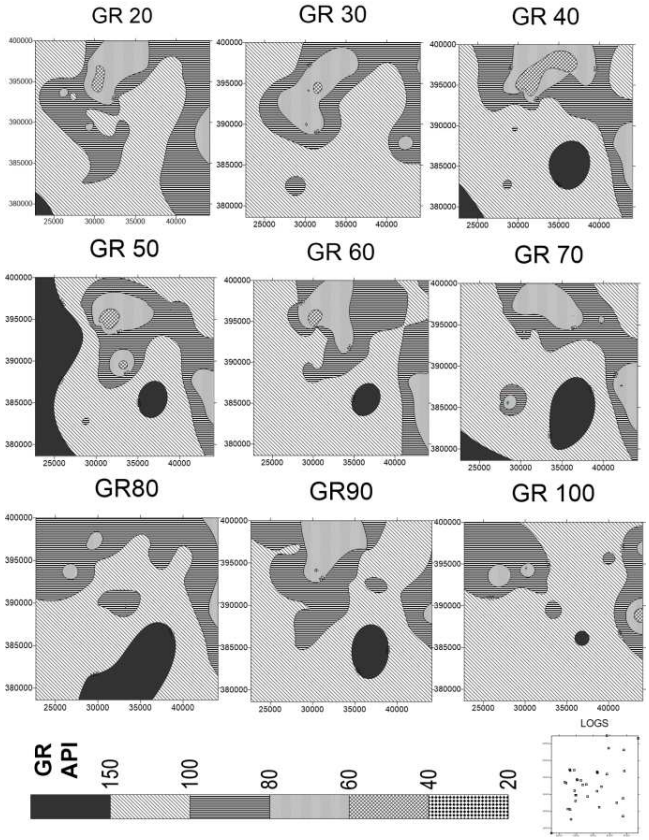

Figure 06. Gamma Ray (GAPI) Electrofacial Composite Maps at each 10 meters depth.

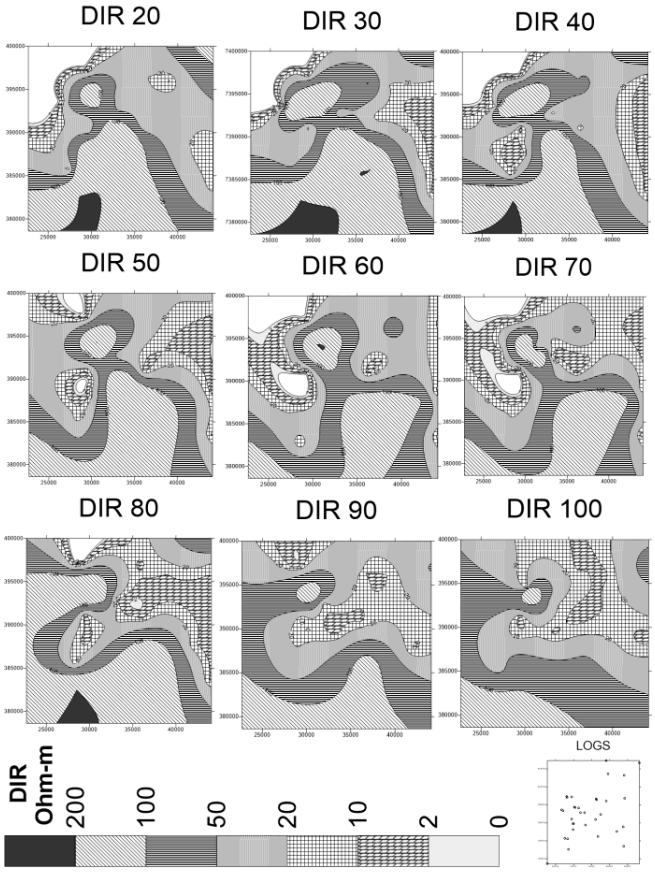

Figure 07 - Transit Time (μs/ft) Electrofacial Composite Maps at each 10 meters depth.

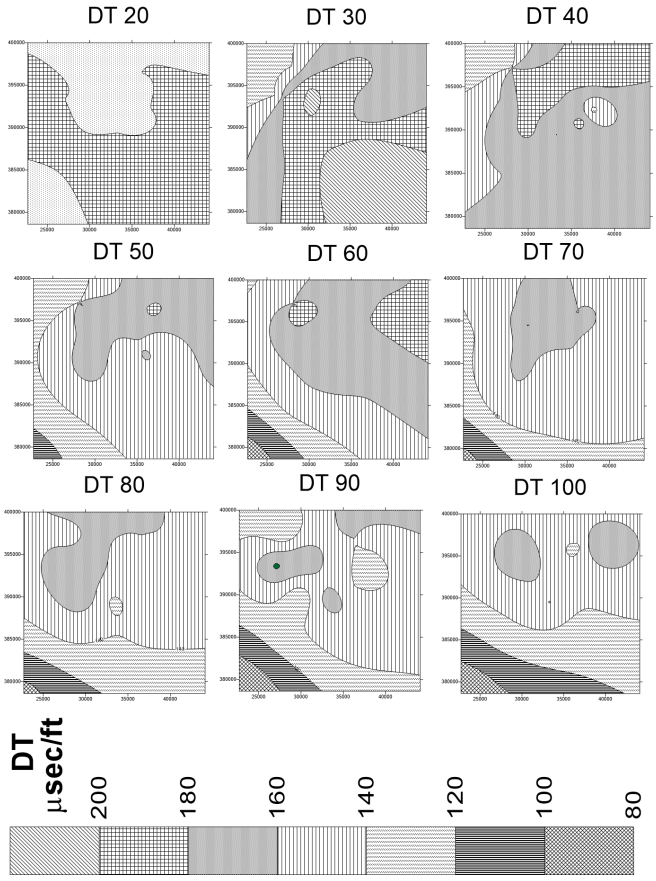

Figure 08 –Deep Induction (ohm.m) Electrofacial Composite Maps at each 10 meters depth.

4.4 *Stratigraphic Section*

The analysis of the curves DIR and GR led to the interpretation of existence of four layers (A, B, C and D) that were identified by results of the log correlation (Figures 9 and 10) with well-defined resistivity characteristics. The upper layer above the layer defined as a layer A represents the changed portion.

The major operational difficulties for the method are: sometimes different lithofacies have similar values in the same type of well log; in the same lithofacies values of a given logs can vary depending on variables such as thickness, pit geometry, texture, etc. Therefore, lithofacies recognition becomes more effective when it employs statistical techniques to allow simultaneous analysis of several logs.

4.4.1 *Layer A*

The layer A has a maximum thickness of 15m and has characteristic resistivity peak. Moreover, the lithology is composed of immature sandstone, with low gamma ray values, with occasional spikes due to the presence of potassium feldspar (arkosic sandstone). This layer when below the water level is a good groundwater catchment.

4.4.2 *Layer B*

The Layer B is the thickest one (40 to 70 meters) and it is composed by shale and clay sediments. Thus, it is no good for groundwater catchment.

4.4.3 *Layer C*

The Layer C is sandier than the layer A and consequently is more favorable to water potential. Its thickness is about 20 meters. In addition, when C is above the crystalline basement, it further increases its water storage.

4.4.4 *Layer D*

The Layer D represents the transition between sediments and crystalline rocks.

5 CONCLUSIONS

The authors do not intend to show a detailed faciological mapping methodology, but rather way to assess the feasibility of the procedures. The major difficult found in São Paulo area was the complexity stratigraphy of the recent sediments in the area. It will be more easy to work in geologically simpler areas, especially where occur mature sandstones without feldspar minerals and also in areas with consolidated materials in a more uniform stratigraphic column.

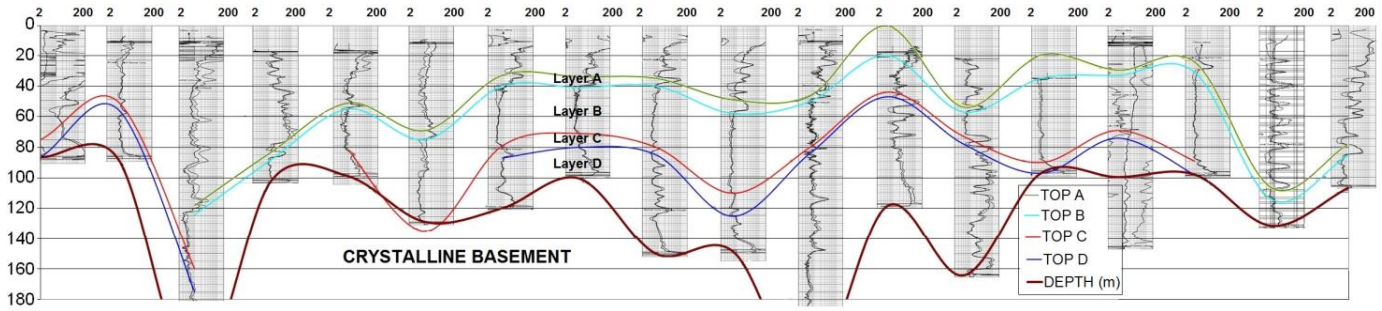

Figure 9. Electrofacies Section NS of study area.

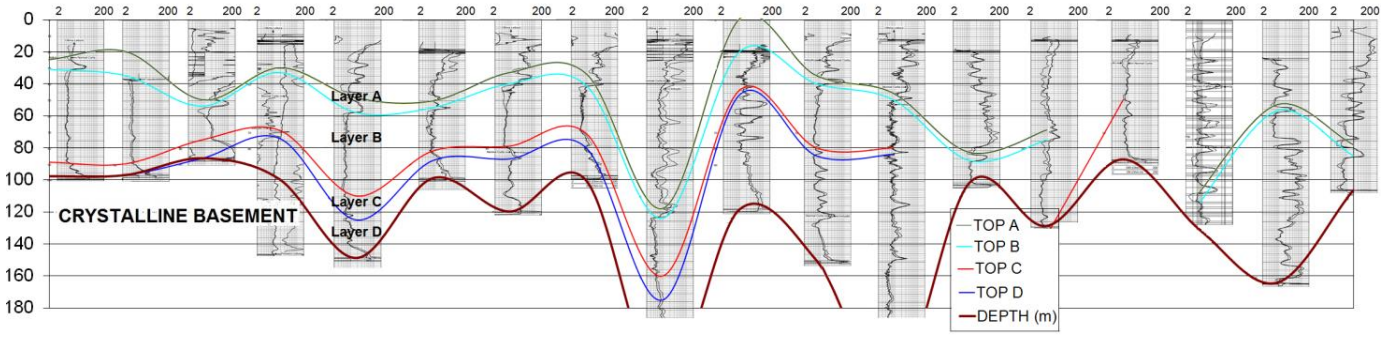

Figure 10. Electrofacies Section EW of study area.

It was possible a better correlation in the business centre area of the map, because of a higher density of logged water wells**.** Although the results showed this methodology can also be applied in areas with comples gelology, they provide a sufficient number of wells to desired detail (design of wells and stratigraphic evaluation).

It can also be interesting to use the same specific software for mining purpose in the data processing to minimize interpolation problems.

6 ACKNOWLEDMENTS

The authors would like to thank the company HYDROLOG Serviços de Perfilagens Ltd for well logs data.

The second author also would like to thank the grants 16/06214-0 and 07/06085-7, São Paulo Research Foundation (FAPESP).

7 REFERENCES

Kearey, P.; Brooks, M. & Hill, I. 2013. An Introduction to Geophysical Exploration. 3rd ed. Oxford: Blackwell Science.

Riccomini, C.; Peloggia, A ; Saloni, J ; Kohnke, M &; Figueira, R. 1989. Neotectonic activity in the Serra do Mar rift system (southeastern Brazil). Journal of South American Earth Sciences JCR, England, v. 2, p. 191-197.

Sturaro, J R; Landim, P. M. B. 1997. Indicator Kriging For Gis'S Maps Integration. Proc. Third Annual Conference of the International Association for Mathematical Geology. Barcelona. Spain International Center for Numerical Methods in Engineering (CIMNE) v. 02, p. 699-704.

Takira, H. 1991. Aplicação dos métodos quantitativos espaciais a dados geológicos da Bacia de São Paulo. M.Sc. Dissertation. Instituto de Geociências da Universidade de São Paulo, São Paulo, 109pp.